

DTIC FILE COPY

NASA  
Technical Memorandum 101460

AVSCOM  
Technical Report 88-C-034

AD-A205 576

# Lubricant Jet Flow Phenomena in Spur and Helical Gears with Modified Addendums— for Radially Directed Individual Jets

Lee S. Akin  
*California State University  
Long Beach, California*

and

Dennis P. Townsend  
*Lewis Research Center  
Cleveland, Ohio*

DTIC  
ELECTE  
MAR 10 1989  
H 8

Prepared for the  
Fifth International Power Transmission and Gearing Conference  
sponsored by the American Society of Mechanical Engineering  
Chicago, Illinois, April 25-27, 1989

**NASA**



DISTRIBUTION STATEMENT A

Approved for public release;

with unlimited distribution

89

3

09

07

LUBRICANT JET FLOW PHENOMENA IN SPUR AND HELICAL GEARS WITH MODIFIED  
ADDENDUMS - FOR RADially DIRECTED INDIVIDUAL JETS

Lee S. Akin  
California State University  
Long Beach, California 90815

and

Dennis P. Townsend  
National Aeronautics and Space Administration  
Lewis Research Center  
Cleveland, Ohio 44135

ABSTRACT

This paper develops the mathematical relations for the "Virtual Kinematic Model" as an improvement over the vectorial model developed earlier. The model solution described herein provides the most energy efficient means of cooling gears - that is, it requires the least pressure or pumping power to distribute the coolant on the tooth surface. Further, this nozzle orientation allows impingement to the root of the tooth if needed and provides the most cooling control when compared to into-mesh or out-of-mesh cooling.

NOMENCLATURE

a	addendum of tooth	$R_t$	transverse pitch radius
$d_i$	impingement depth	$R_x$	uncorrected radius at impingement point (see Fig. 3)
$d_x$	uncorrected impingement depth in origin plane	t	arbitrary flight time
ev	of $\theta = \sec \phi =$ evolvent function of $\theta$	$t_f$	jet stream flight time at impingement
N	number of teeth in gear	$t_w$	time to rotate through angle, $\theta_w$
n	rotational speed	$V_g$	linear pitch line velocity of gear
$P_d$	diametrical pitch	$V_j$	jet velocity
$P_n$	normal diametrical pitch	$\alpha$	jet inclination angle
$P_t$	transverse diametrical pitch	$\Delta a$	addendum modification
R	standard pitch radius	$\delta_i$	dimensionless impingement depth $\frac{d_i P_d}{2}$
$R_b$	base radius of gear	$\epsilon_{iv}$	virtual roll angle at impingement point
$R_{bv}$	base radius of virtual involute	$\epsilon_{ov}$	virtual roll angle to outside diameter
$R_i$	radius at impingement point	$\theta_a$	vectorial angle of involute between point i and O (Fig. 2)
$R_{or}$	operational outside radius (for modified addendum)	$\theta_i$	involute of $\phi_i =$ involute function at impingement point
$R_o$	standard outside radius	$\theta_{iv}$	virtual vectorial angle to impingement point
		$\theta_{ov}$	virtual vectorial angle to outside diameter
		$\theta_r$	angle across tooth space at base circle
		$\theta_w$	total vectorial angle at impingement point
		$v_j$	dimensionless jet velocity $V_j/V_g$
		$\rho_b$	dimensionless base circle radius
		$\rho_i$	dimensionless impingement radius

$\rho_{or}$  dimensionless outside radius  
 $\rho_t$  dimensionless transverse pitch radius  
 $\phi$  pressure angle at pitch radius  
 $\phi_i$  pressure angle at impingement point  
 $\phi_{iv}$  pressure angle of virtual involute at impingement point  
 $\phi_n$  normal pressure angle  
 $\phi_o$  pressure angle at outside radius  
 $\phi_{ov}$  pressure angle of virtual involute at outside diameter  
 $\phi_t$  transverse pressure angle  
 $\psi$  helical angle  
 $\omega_g$  gear angular velocity  
 $\omega_j$  virtual jet angular velocity

## INTRODUCTION

Cooling of lightweight high speed gears via the lubricating oil supply provided to the gearbox continues to be one of the most difficult areas in the high performance mechanical power transmission design process. Since the cooling process is controlled by oil jet orientation and by the jet velocity relative to the pitch line velocity (PLV), these authors have considered the development of a fundamental understanding of the oil jet primary impingement phenomena as essential to understanding how the gear tooth cooling process works. In the early 1970's when this work was started, a "vectorial model" was used to describe the radial jet flow phenomena, (Akin, 1975), which compared reasonably well with the experimental data, (Akin, 1975), especially at pressures above approximately 140 kPa (20 psi). Models were also developed for into mesh (Akin, 1983) and for out of mesh (Akin, 1985) to determine the oil jet impingement depths for these conditions. The into mesh and out of mesh models indicate the oil jet impingement depths were limited and therefore maximum cooling could not be obtained using this approach.

The "Virtual Kinematic Model" was first mentioned by Townsend in 1980, but the full mathematical development of this model has not been published until now. This model has been generalized to include spur or helical gears with standard AGMA proportions as well as long or short addendums. Further, parametric limitations have been formulated to allow the gear analyst to know he is specifying his problem where a solution is possible. Also, the dimensionless parameter development has been provided to allow the gear engineer to examine a wide range of generalized solutions easily and to expose the limits mentioned above.

## KINEMATIC SOLUTION FOR MODIFIED SPUR GEARS

The jet stream flight time starts ( $t = 0$ ) at position "1" at the intersection of the top land and trailing profile of the leading tooth, as shown in Fig. 1. Then the terminal end of the jet passes through the tooth space where it impinges at "i" on the leading profile of the trailing tooth at radius

$R_i$  after time ( $t = t_f$ ). From inspection of Fig. 1, it can be seen that the radius of impingement is:

$$R_i = R_o - V_j t_f \quad (1)$$

where  $V_j$  is the jet velocity. The time of flight of the oil jet through the tooth space is:

$$t_f = \frac{R_o - R_i}{V_j} = \frac{d_i}{V_j} \quad \text{sec} \quad (2)$$

The gear must rotate through the angle  $\theta_w$  in the same time it takes the oil jet to travel through the tooth space to a depth of  $d_i = V_j t_f$  and impinge at  $R_i$ . From Fig. 1 we see that  $\theta_w = \theta_o + \theta_r + \theta_i$ . The components of  $\theta_w$  are developed below.

The pressure angle,  $\phi_i$ , at the depth of impingement,  $d_i$  is:

$$\phi_i = \cos^{-1}\left(\frac{R_b}{R_i}\right) \text{ and } \tan \phi_i = \left[\frac{R_i^2}{R_b^2} - 1\right]^{1/2} \quad (3)$$

where

$R_b$  is the gear base radius

$$R_i = R_o - d_i$$

so that  $\theta_i = \text{inv } \phi_i = \tan \phi_i - \phi_i$ .

Also, the angle across the tooth space at the gear base circle is:

$$\theta_r = \frac{\pi}{N} - 2 \text{ inv } \phi = \frac{\pi}{N} - 2(\tan \phi - \phi) \quad (4)$$

where  $\phi = \cos^{-1}(R_b/R)$  is the pressure angle at the standard pitch circle  $R$ . Further, the pressure angle at the outside radius  $R_o$  is:

$$\phi_o = \cos^{-1}\left(\frac{R_b}{R_o}\right) \text{ and } \tan \phi_o = \left[\frac{R_o^2}{R_b^2} - 1\right]^{1/2} \quad (5)$$

so that

$$\theta_o = \text{inv } \phi_o = \tan \phi_o - \phi_o$$

and thus

$\theta_w = \theta_o + \theta_r + \theta_i$  as stated earlier, so that the time it takes the gear to rotate through  $\theta_w$  is

$$t_w = \frac{\theta_w}{\omega_g} = \frac{30 \theta_w}{\pi n} \quad \text{sec} \quad (6)$$

where  $n = \text{rev/min}$ .

Equating the times of flight  $t_f$  and rotation  $t_w$ :

$$\frac{d_i}{V_j} = \frac{30 \theta_w}{\pi n} \quad \text{or} \quad \frac{R_o - R_i}{V_j} = \frac{\theta_w}{\omega_g} \quad (7)$$

If  $d_i$  is given, then the required  $V_j$  can be found explicitly as

$$V_j = \frac{\omega_g d_i}{\theta_w} = \frac{\pi d_i n}{30 \theta_w} \quad (8)$$

note, that  $d_i$  is a function of  $\phi_i$  ( $d_i = f_n(\phi_i)$ )

If  $V_j$  is given and the resulting  $d_i$  or  $R_i$  is desired, we must iterate until  $R_i$ , as  $fn(\phi_i, V_j)$ , is satisfied. In dimensionless form, where:  
 $v_j = V_j/V_g$  and  $\delta_i = d_i P_d/2$

$$v_j = \frac{d_i}{R_o \theta_w} = \frac{4 \delta_i}{[(N+2)\theta_w]} \quad (9)$$

GEARS WITH MODIFIED ADDENDUMS AND AN OIL JET DIRECTED AT AN ARBITRARY INCLINATION ANGLE  $\alpha$  FROM THE GEAR CENTER

A more general solution can be provided to this problem if we assume that the jet is pointed away from the line through center of the gear by an arbitrary angle " $\alpha$ " as shown in Fig. 2. This angle is defined to be positive in magnitude when pointed in the direction of  $\omega_g$  as shown in Fig. 2. Modified addendum lengths or center distances are accommodated by the use of the parameter  $\Delta R_o = \Delta N_g/2 P_n = \Delta a$ , so that  $R_{or} = R_o + \Delta a$ . Obviously when  $\Delta a = 0$ ,  $R_o = R_{or}$ . In this paper we will generalize and use  $\Delta a$ ,  $R_o$ , and  $R_{or}$  in all equations.

For helical gears we let:  $R_t = N(2P_n \cos \psi)$ , so that,  $R_o = R_t + a$  and  $R_{or} = R_t + a + \Delta a$ , where  $P_t = P_n \cos \psi$  and the subscript  $t$  refers to the transverse plane (normal to gear axis.) This problem has been formulated by assuming that the jet terminal end (or head) follows a trajectory in mesh with a "virtual involute" as shown in Fig. 2. The virtual involute is: defined by the radius of the base circle  $R_{bv}$ , where

$$R_{bv} = R_{or} \sin \alpha, \quad V_j = \omega_j R_{bv}, \quad \text{or} \quad \omega_j = \frac{V_j}{R_{or} \sin \alpha} \quad (10)$$

As can be seen by inspection of Fig. 2, " $\omega_j$ " is the theoretical angular velocity of the virtual jet involute that produces the proper locus for the terminal end of the jet stream line at the actual jet velocity  $V_j$ , subsequent to passing the point 1 at  $t = 0$ . The virtual involute is used to develop the mathematical relationships needed to formulate the time of flight to impingement of the jet stream on the trailing tooth profile at  $R_i$  when the gear angular velocity is  $\omega_g$ . Note that in general  $\omega_g \neq \omega_j$  since the virtual base circle is not fixed on the gear blank (or wheel).

The writer has selected the virtual involute generalized roll angle  $\epsilon_v$  as the parameter to interrelate the virtual involute for the jet stream with the rotating gear geometry. Thus the virtual roll angle  $\epsilon_{ov}$  at the gear outside diameter can be calculated from the fundamental relationship (see Fig. 2):

$$R_{bv} \epsilon_{ov} = R_{or} \cos \alpha, \text{ so that } \epsilon_{ov}$$

$$= \frac{R_{or} \cos \alpha}{R_{bv}} = \frac{R_{or} \cos \alpha}{R_{or} \sin \alpha} = \frac{1}{\tan \alpha} = \cot \alpha \quad (0 < \alpha < \frac{\pi}{2}) \quad (11)$$

From here we can develop the remainder of the virtual involute functions including  $\theta_{ov}$  and  $\phi_{ov}$  as follows (see Fig. 2):

$$\epsilon_{ov} = (\text{ev}^2 \theta - 1)^{1/2} \text{ or } \text{ev} \theta = (\epsilon_{ov}^2 + 1)^{1/2} \text{ where by definition (Vogel, 1945):}$$

$\text{ev} \theta = R_{or}/R_{bv}$ , so that  $\epsilon_{ov} = [(R_{or}/R_{bv})^2 - 1]^{1/2}$  avoids the use of  $\alpha$  functions. The virtual vectorial angle or polar angle  $\theta_{ov}$  at the O.D. is:

$$\theta_{ov} = [R_{or}/R_{bv}]^2 - 1]^{1/2} - \tan^{-1} [(R_{or}/R_{bv})^2 - 1]^{1/2} \quad (\text{rad.}) \text{ and the virtual pressure angle } \phi_{ov} \text{ is obtained from:}$$

$$\phi_{ov} = \text{inv}^{-1} \theta_{ov} = \sec^{-1} (\text{ev} \theta_{ov}) = \cos^{-1} (R_{bv}/R_{or}). \quad (12)$$

From the above we get  $\epsilon_{ov} = \epsilon_{ov} + \phi_{ov}$  as a check.

Also,  $\alpha = \alpha_{ov} = \pi/2 - \phi_{ov}$  (rad) as a check)

$$\epsilon_{ov} = \frac{R_{or} \cos \alpha}{R_{bv}} = \cot \alpha \quad (0 < \alpha < \frac{\pi}{2}) \quad (13)$$

The virtual roll angle  $\epsilon_{iv}$  at the impingement diameter is developed as follows:

$$\epsilon_{o-i} = \epsilon_{ov} - \epsilon_{iv} = \omega_j t_f = \frac{V_j t_f}{R_o \sin \alpha} \quad (14)$$

$$\text{so that } \epsilon_i(t_f) = \epsilon_{ov} - \omega_j t_f = (R_{or} \cos \alpha - V_j t_f) / (R_{or} \sin \alpha) = \cot \alpha - V_j t_f / (R_{or} \sin \alpha).$$

Note from Fig. 2 that  $V_j t_f = d_i / \cos \alpha$ , thus when  $V_j$  and/or  $t_f$  are unknown:

$$\begin{aligned} \epsilon_{iv}(d_i) &= \frac{R_{or} \cos \alpha - \frac{d_i}{\cos \alpha}}{R_{or} \sin \alpha} = \cot \alpha - \frac{d_i}{R_{or} \sin \alpha \cos \alpha} \\ \text{and } \epsilon_{o-i} &= \epsilon_{ov} - \epsilon_{iv} \\ &= \cot \alpha - \cot \alpha + \frac{d_i}{R_{or} \sin \alpha \cos \alpha} = \frac{2d_i}{R_{or} \sin 2\alpha} \quad (15) \end{aligned}$$

Again the other virtual involute functions at the impingement diameter are; starting with the vectorial angle:

$$\theta_{iv} = \left[ \frac{(R_{or} - d_i)^2}{R_{bv}^2} - 1 \right]^{1/2} - \tan^{-1} \left[ \frac{(R_{or} - d_i)^2}{R_{bv}^2} - 1 \right]^{1/2} \quad (\text{rad.}) \quad (16)$$

and the virtual pressure angle  $\phi_{iv}$  at  $R_i$ :

A-1

$$\phi_{iv} = \cos^{-1} \left[ \frac{R_{bv}}{R_{or} - d_i} \right] \quad (17)$$

Further noting that

$$e_{iv} = \left[ \frac{(R_{or} - d_i)^2}{R_{bv}^2} - 1 \right]^{1/2} = \phi_{iv} + \theta_{iv} \text{ as a check, and} \quad (18)$$

$$\alpha_{iv} = \frac{\pi}{2} - \phi_{iv} \text{ (rad.) and } R_i = R_{bv} (e_{iv}^2 + 1)^{1/2}$$

as a check. Thus the time of flight can be checked from:

$$t_f = \frac{e_{iv}}{\omega_j} = \frac{d_i}{R_{or} \sin \alpha \cos \alpha [V_j / (R_{or} \sin \alpha)]} = \frac{d_i}{V_j \cos \alpha} \text{ (sec)} \quad (19)$$

where

$$d_i = (R_o + \Delta a) - R_i = R_{or} - R_i$$

Theoretically, the virtual involute is a dummy device for mathematically describing the time motion of the terminal end of the jet stream line. As such, the jet stream line is the line of action between the virtual involute and the oil jet. Thus the coincident points "i" at radius  $r_i$  on the virtual involute (v.i.) and  $R_i$  on the gear tooth (g.t.) define the point of oil impingement at time  $t_f$  (v.i.) =  $t_w$  (g.t.). This coincident instant in time is the result of the simultaneous motions of the (v.i.) and (g.t.) from time  $t = 0$  when the (v.i.) is at its outer position 2 at the virtual base circle (Fig. 2) while the trailing edge of the leading gear tooth is at position "0" where the jet line crosses the O.D. and the (v.i.) is such that the rotation of the (v.i.) at  $\omega_g$  without the relative rotation of  $(\omega_j - \omega_g)$  through time  $t_w$  would place the (v.i.) origin at position 3 at the virtual base circle. Thus the (v.i.) is perceived to rotate faster than  $\omega_j$  by the amount  $(\omega_j - \omega_g)$  such that it rotates at  $\omega_g + (\omega_j - \omega_g) = \omega_j$  in keeping with the jet velocity  $V_j$  which places the (v.i.) at position 4 at the virtual base circle and at i on the leading profile of the trailing tooth as shown in Fig. 2

It is now necessary to involve the gear tooth geometry. The solution will involve the assumption

$$r_i = R_i = R_{or} - d_i$$

where

$$d_i = V_j t_f \cos \alpha \quad (20)$$

Thus from the geometry of Fig. 2 it can be seen that  $\theta_a$  can be approximated from:

$$\tan \theta_a = \frac{V_j t_f \sin \alpha}{R_{or} - V_j t_f \cos \alpha} = \frac{d_i \tan \alpha}{R_{or} - d_i} = \frac{(R_{or} - R_i) \tan \alpha}{R_i} \quad (21)$$

However, we cannot use  $d_i$  to calculate  $\theta_a$  except as an approximation because the angular origin for  $\theta_a$  is along the radius vector  $R_x$  (Fig. 3) passing through the time origin at "0" while  $d_i$  is measured along the  $R_i$  radius vector terminating at point "i" on the leading profile of the trailing tooth, which is the terminating vector position for the angle  $\theta_a$ ; thus (see Fig. 3):

$$R_x = R_i \cos \theta_a = (R_{or} - d_i) \cos \theta_a \quad (22)$$

$$d_x = R_{or} - R_x = R_{or} - (R_{or} - d_i) \cos \theta_a \quad (\text{See Fig. 3})$$

Noting that:

$$d_x \tan \alpha = R_x \tan \theta_a \quad (23)$$

it can be shown that:

$$d_x = R_{or} \cos \alpha - [(R_{or} \cos \alpha)^2 - d_i(2R_{or} - d_i)]^{1/2} \cos \alpha. \quad (24)$$

so that,  $\theta_a = \tan^{-1} [d_x \tan \alpha / (R_{or} - d_x)]$ .

Then as a check on the calculated value of  $d_x$  above:

$$d_i = R_{or} - \frac{R_{or} - d_x}{\cos \theta_a} \quad (25)$$

which should be the same as before.

If it is noted that  $R_i = R_{or} - d_i$  then (see Fig. 2).

$$\theta_i = \text{inv } \phi_i = \tan \phi_i - \phi_i = \left[ \left( \frac{R_i}{R_b} \right)^2 - 1 \right]^{1/2} - \cos^{-1} \left( \frac{R_b}{R_i} \right) \quad (26)$$

Note that  $\phi_i$  is a function of  $R_i$  and  $d_i$  making an explicit solution for  $(R_i$  or  $d_i)$  impossible when  $V_j$  is specified leaving  $d_i$  or  $R_i$  as the dependent variable. Also.

$$\theta_r = \frac{\pi}{N} - \frac{4\Delta a \tan \phi_n}{R} - 2\theta_n \quad (27)$$

where:  $\theta_n = \text{inv } \phi_n = \tan \phi_n - \phi_n$  for spur gears and

$\theta_r = \pi/n - 2\Delta a \tan \phi_t / R_t - 2\theta_t$  for helical gears

where

$$\theta_t = \text{inv } \phi_t = \tan \phi_t - \phi_t \text{ and } \tan \phi_t = \tan \phi_n \sec \psi$$

$$\text{and } R_t = \frac{N}{2P_t} \quad (28)$$

Further

$$\theta_o = \tan \phi_o - \phi_o = \left[ \left( \frac{R_{or}}{R_b} \right)^2 - 1 \right] - \cos^{-1} \left( \frac{R_b}{R_{or}} \right) \quad (29)$$

Now the gear angle of rotation,  $\theta_w$ , between points 1 and i in Fig. 2, can be calculated from

$$\theta_w = \theta_o + \theta_r + \theta_i + \theta_a \quad (30)$$

so that

$$t_w = \frac{\Theta_w}{\omega_g} = \frac{30(\Theta_o + \Theta_r + \Theta_i + \Theta_a)}{\pi n} \text{ sec} \quad (31)$$

where

$$n = \text{rev./min}$$

It is now possible to equate the time of flight  $t_f$  of the oil jet to the time of gear rotation  $t_w$ , so that

$$t_w(\text{g.t.}) = \frac{30\Theta_w}{\pi n} = \frac{d_i}{(V_j \cos \alpha)} = t_f(\text{v.i.}) \quad (32)$$

Since  $\Theta_i$  is  $\text{fn}(d_i)$ , the impingement depth cannot be solved explicitly but must be iterated numerically. Thus, we solve for  $V_j$  so that an explicit solution is possible as follows:

$$V_j = \frac{\pi d_i n}{30\Theta_w \cos \alpha} = \frac{d_i \omega_g}{\Theta_w \cos \alpha} \quad (33)$$

It would be desirable to graph the results of these formulas as in Figs. 4 and 5. Thus the independent variables will be normalized to provide dimensionless solutions to the above results. The principle parameters used are  $V_j$  and  $d_i$  so that we will express them in terms of the dimensionless parameters  $v_j$ ,  $\delta_i$  and  $N$  as:

$$v_j = \frac{V_j}{V_g} = \frac{V_j}{\omega_g R_{or}} = \frac{d_i}{\Theta_w R_{or} \cos \alpha} \quad (34)$$

and

$$V_j = v_j \omega_g R_{or} \delta_i = \frac{d_i}{W.D.} = \frac{d_i}{2/P_n} = \frac{d_i P_n}{2} \quad \text{and} \quad d_i = \frac{2\delta_i}{P_n} \quad (35)$$

where W.D. is the whole depth.

Thus the time of flight ( $t_f$ ) from the trailing edge of the leading tooth top land at radius  $R_{or}$  to the radius of impingement  $R_i$  on the leading profile of the trailing tooth is:

$$t_f = \frac{2\delta_i}{v_j \omega_g P_n R_{or} \cos \alpha} \quad (36)$$

and in terms of  $N$ , using  $R_{or} = (N + 2 \cos \psi + 2\Delta n)/(2P_n \cos \psi)$ :

$$t_f = \frac{4\delta_i \cos \psi}{[v_j \omega_g (N + 2 \cos \psi + 2\Delta n) \cos \alpha]} \quad (37)$$

Then the time of rotation  $t_w$  from the trailing edge of the leading tooth top land at radius  $R_{or}$  to the jet line when it intercepts the impingement point at radius  $R_{or}$  on the leading profile of the trailing tooth is:

$$t_w = \frac{\Theta_w}{\omega_g} \quad (38)$$

where

$$\Theta_w = \Theta_o + \Theta_r + \Theta_i + \Theta_a \quad (39)$$

so that angular geometry expressed in fundamental terms of  $N$ ,  $\Delta N$ ,  $\phi$ ,  $\psi$ ,  $\alpha$  and  $\delta_i$  or  $v_j$  are; starting with the vectorial angle  $\Theta_a$  (see Fig. 1) is:

$$\tan \Theta_a = d_i \tan \frac{\alpha}{R_i}, \text{ so that}$$

$$\Theta_a = \tan^{-1} \left[ \frac{4\delta_i \tan \alpha \cos \psi}{N + 2 \cos \psi + 2 \Delta N - 4\delta_i \cos \psi} \right] \quad (40)$$

Next the impingement angle  $\Theta_i$  (see Fig. 1) is:

$$\Theta_i = \tan \phi_i - \phi_i = \left( \frac{p_i^2}{p_b^2} - 1 \right)^{1/2} - \cos^{-1} \left( \frac{p_b}{p_i} \right) \quad (41)$$

where

$$p_i = 1 - \frac{4\delta_i \cos \psi}{N + 2\Delta N + 2 \cos \psi}$$

$$p_b = \frac{N \cos \phi_t}{N + 2\Delta N + 2 \cos \psi}$$

thus

$$\left( \frac{p_i}{p_b} \right) = \frac{((N + 2 \cos \psi + 2\Delta N) - 4\delta_i \cos \psi)}{N \cos \phi_t} \quad (42)$$

and

$$p_{or} = 1$$

Now this is valid only when ( $N$  is given):

$$\delta_i \leq \frac{N + 2\Delta N + 2 \cos \psi - N \cos \phi_t}{4 \cos \psi} = \delta_i(\text{max}) \quad (43)$$

or when  $\delta_i$  is given

$$N \geq 2 \left[ \frac{(2\delta_i - 1) \cos \psi - \Delta N}{1 - \cos \phi_t} \right] = N(\text{min}) \quad (44)$$

the tooth space angle  $\Theta_r$  at the base diameter is

$$\Theta_r = \frac{\pi}{N} - \frac{4\Delta N}{N} \tan \phi_t - 2\Theta_t \quad (45)$$

where

$$\Theta_t = \tan \phi_t - \phi_t - \left[ \left( \frac{p_t}{p_b} \right)^2 - 1 \right]^{1/2} - \cos^{-1} \frac{p_b}{p_t} \quad (46)$$

where

$$P_t = \frac{N}{N + 2 \cos \psi + 2\Delta N}$$

and

$$\frac{P_t}{P_b} = \frac{1}{\cos \phi_t} = \sec \phi_t$$

and finally the involute angle  $\theta_o$  to the outside diameter is:

$$\theta_o = \text{inv } \phi_{or} = \tan \phi_{or} - \phi_{or} = \left( \frac{1}{P_b} - 1 \right)^{1/2} - \cos^{-1} (P_b) \quad (47)$$

again it is possible to equate the times of flight  $t_f$  and rotation  $t_w$ , now in terms of dimensionless parameters, so that

$$\frac{\theta_w}{\omega_g} = \left[ \frac{4 \delta_i \cos \psi}{v_j (N + 2 \cos \psi + 2\Delta N) \cos \alpha} \right] \quad (48)$$

Therefore, if the dimensionless depth  $\delta_i \leq \delta_i(\max)$  is given the dimensionless velocity is calculated from:

$$v_j = \left[ \frac{4 \delta_i \cos \psi}{\theta_w (N + 2 \cos \psi + 2\Delta N) \cos \alpha} \right] \quad (49)$$

Also, if the dimensionless velocity  $v_j$  is given then the dimensionless depth  $\delta_i$  is:

$$\delta_i = \frac{\theta_w v_j (N + 2 \cos \psi + 2\Delta N) \cos \alpha}{4 \cos \psi} \quad (50)$$

where the limits for  $\delta_i$  and/or  $N$  from Eqs. 43 and 44 must be observed.

Further, solving for  $\delta_i$  must be done by an iteration technique since  $\theta_w(\delta_i)$  is a function of  $\delta_i$  and is therefore not explicit.

#### RESULTS OF COMPUTERIZED PARAMETRIC STUDIES

As noted in the introduction a completely new analytical approach has been taken to development of the mathematical model for what we identify as the Kinematic model.

The effect of inclination angle ( $\alpha$ ) in the Kinematic model is shown in Fig. 4 which is in keeping with the physics of the problem. It should be noted here that windage has been neglected in keeping with the results from previous studies (Akin, 1975).

It should also be noted that when fan jets are used and are oriented with the fan perpendicular or broadside to the direction of flow around the gear, the resulting impingement depth will probably compare better with a curve for a slightly larger inclination angle than indicated by the pointing direction of the

jet nozzle. Also the effect of jet velocity on depth  $\delta_i$  is shown in Fig. 5. The curve presented here is for a specific gear design: pressure angle  $\phi = 20^\circ$ , number of teeth  $N = 28$ , inclination angle  $\alpha = 47^\circ$ , and dimensionless jet velocity  $V_j/V_g = v_j = 0.6468$ .

Figure 6 (Akin, 1975) shows the theoretical results compared with the experimental data gathered in 1974. The experimental data did lie substantially below the prediction from the mathematical models at low oil pressures. It is assumed, as also mentioned earlier, that this is the result of (1) the windage effect on a fan-jet at low jet velocity and (2) pressure loss in the nozzle. As the jet velocity is increased the experimental data approaches the curves. The windage study conducted in Akin (1975) involved predicting the trajectory of the oil droplets after they passed into the tooth space between the gear teeth. Under these circumstances the windage effect is considered negligible except for small droplet sizes around 0.001 cm (0.0004 in.).

#### CONCLUSION

This paper develops the mathematical relations for the "Virtual Kinematic Model" as an improvement over the vectorial model developed earlier. The model solution described herein provides the most energy efficient means of cooling gears—that is, it requires the least pressure or pumping power to distribute the coolant on the tooth surface. Further this nozzle orientation allows impingement to the root if needed and provides the most control when compared to the into-mesh or out-of-mesh cooling.

#### REFERENCES

- Akin, L.S. and Mross, J.J., 1975, "Theory for the Effect of Windage on the Lubricant Flow in the Tooth Spaces of Spur Gears," Journal of Engineering for Industry, Vol. 97, No. 4, pp. 1266-1273.
- Akin, L.S. and Townsend, D.P., 1983, "Into Mesh Lubrication of Spur Gears with Arbitrary Offset Oil Jet. Part 1: For Jet Velocity Less Than or Equal to Gear Velocity," Journal of Mechanisms, Transmissions, and Automation in Design, Vol. 105, No. 4, pp. 713-718.
- Akin, L.S. and Townsend, D.P., 1983, "Into Mesh Lubrication of Spur Gears with Arbitrary Offset Oil Jet. Part 2: For Jet Velocities Equal to or Greater than Gear Velocity," Journal of Mechanisms, Transmissions, and Automation in Design, Vol. 105, No. 4, pp. 719-724.
- Akin, L.S. and Townsend, D.P., 1985, "Lubricant Jet Flow Phenomena in Spur and Helical Gears with Modified Center Distances and/or Addendums - For Out-of-Mesh Conditions," Journal of Mechanisms, Transmissions, and Automation in Design, Vol. 107, No. 1, pp. 24-30.
- Akin, L.S., Townsend, D.P., and Mross, J.J., 1975, "Study of Lubricant Jet Flow Phenomena in Spur Gears," Journal of Lubrication Technology, Vol. 97, No. 2, pp. 283-288, 295.
- Townsend, D.P. and Akin, L.S., 1981, "Analytical and Experimental Spur Gears Tooth Temperature as Affected by Operating Variables," Journal of Mechanical Design, Vol. 103, No. 4, pp. 219-226.
- Vogel, W.F., 1945, Involutes and Trigonometry, Michigan Tool Co., Detroit, MI.

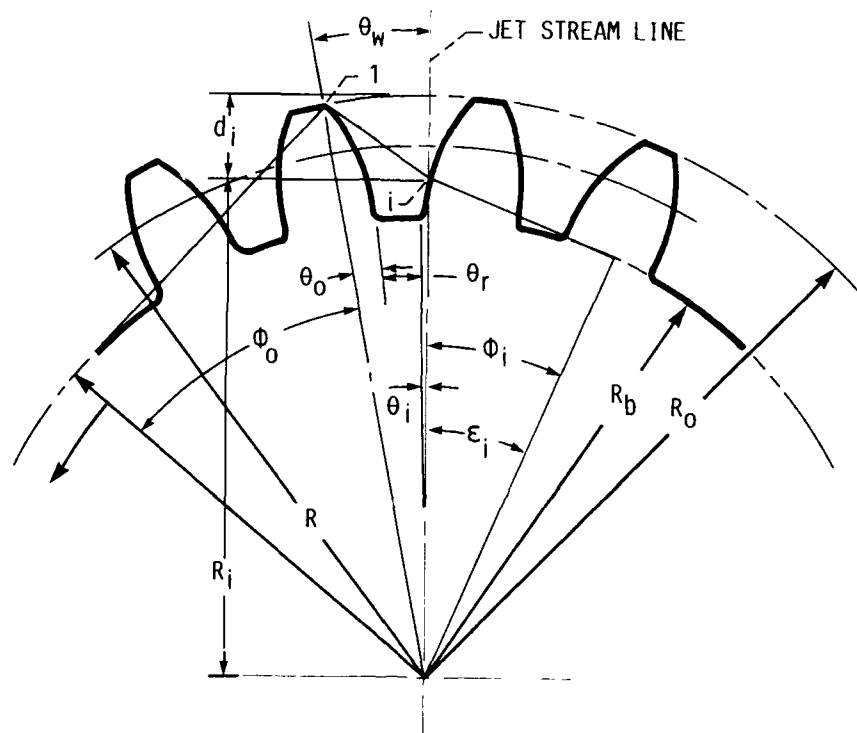


FIGURE 1. - KINEMATIC MODEL WITH RADIAL JET.



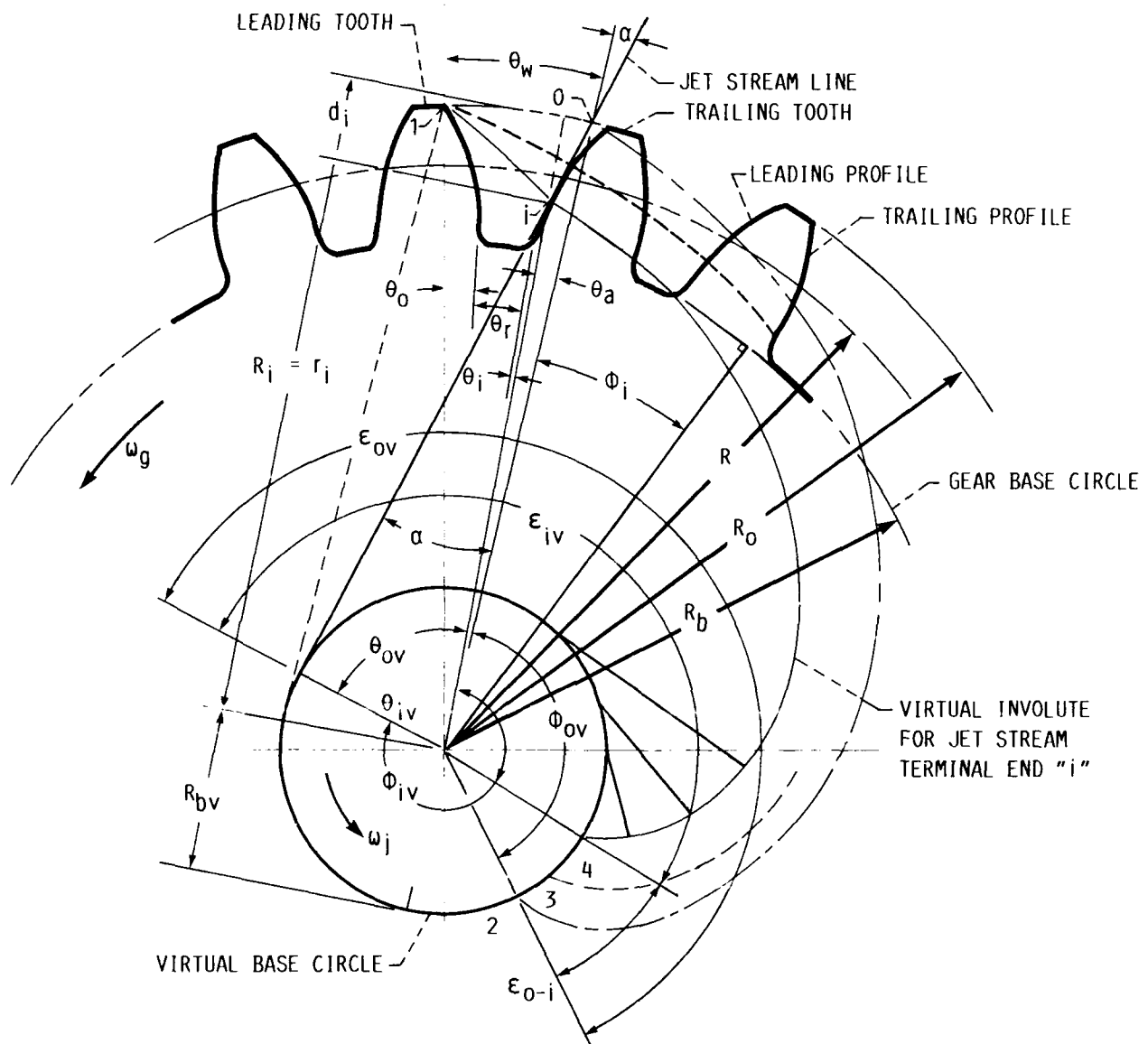


FIGURE 2. - KINEMATIC MODEL WITH ARBITRARY INCLINATION ANGLE " $\alpha$ ".

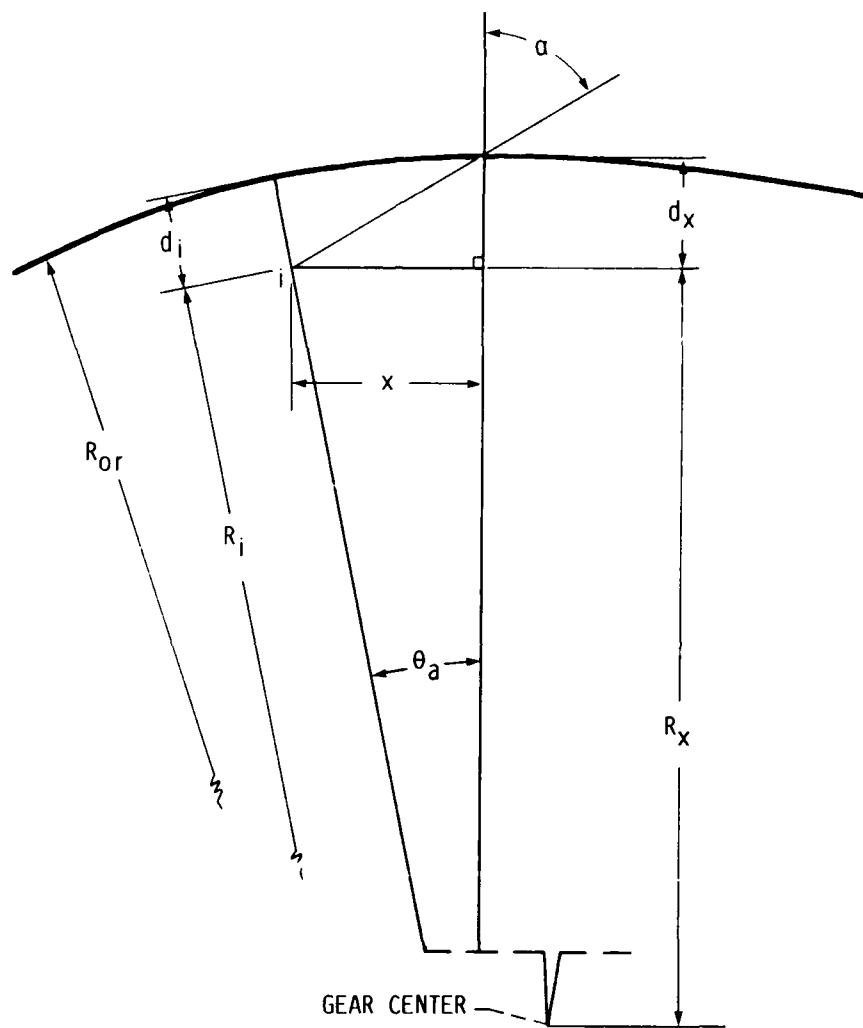


FIGURE 3. - ENLARGED DETAIL OF KINEMATIC MODEL TO SHOW GEOMETRY CORRECTION FOR  $d_i$  AS A RESULT OF  $\theta_a$ .

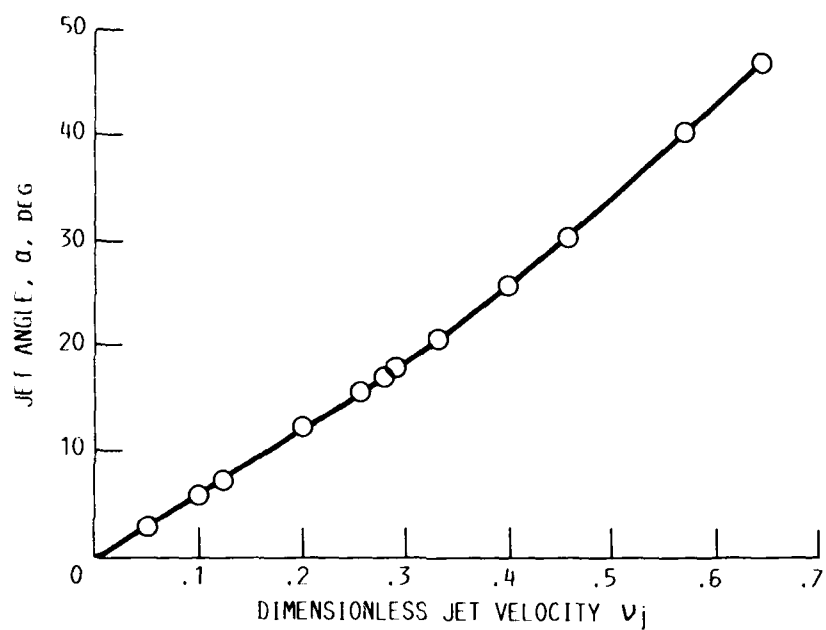


FIGURE 4. - JET ANGLE  $\alpha$  WHICH GIVES MAXIMUM DIMENSIONLESS DEPTH OF IMPINGEMENT  $\delta_i$  FOR A GIVEN DIMENSIONLESS JET VELOCITY  $v_j$ .



## Report Documentation Page

1 Report No NASA TM-101460 AVSCOM TR-88-C-034	2. Government Accession No	3. Recipient's Catalog No.	
4 Title and Subtitle Lubricant Jet Flow Phenomena in Spur and Helical Gears with Modified Addendums—for Radially Directed Individual Jets		5. Report Date	
		6. Performing Organization Code	
7 Author(s) Lee S. Akin and Dennis P. Townsend		8. Performing Organization Report No. E-4533	
		10. Work Unit No. 505-63-51 1L162209A47A	
9 Performing Organization Name and Address NASA Lewis Research Center Cleveland, Ohio 44135-3191 and Propulsion Directorate U.S. Army Aviation Research and Technology Activity—AVSCOM Cleveland, Ohio 44135-3127		11. Contract or Grant No.	
		13 Type of Report and Period Covered Technical Memorandum	
12 Sponsoring Agency Name and Address National Aeronautics and Space Administration Washington, D.C. 20546-0001 and U.S. Army Aviation Systems Command St. Louis, Mo. 63120-1798		14. Sponsoring Agency Code	
15 Supplementary Notes Prepared for the Fifth International Power Transmission and Gearing Conference sponsored by the American Society of Mechanical Engineers, Chicago, Illinois, April 25-27, 1989. Lee S. Akins, California State University, Long Beach, California 90815 (work funded under NASA Grant NAG3-20) and Dennis P. Townsend, NASA Lewis Research Center.			
16 Abstract This paper develops the mathematical relations for the "Virtual Kinematic Model" as an improvement over the vectorial model developed earlier. The model solution described herein provides the most energy efficient means of cooling gears—that is, it requires the least pressure or pumping power to distribute the coolant on the tooth surface. Further, this nozzle orientation allows impingement to the root of the tooth if needed and provides the most cooling control when compared to into-mesh or out-of-mesh cooling.			
17 Key Words (Suggested by Author(s)) Lubrication; Gears; Cooling; Oil jet flow; Gear geometry.		18. Distribution Statement Unclassified—Unlimited Subject Category 37	
19 Security Classif. (of this report) Unclassified	20. Security Classif. (of this page) Unclassified	21. No of pages 12	22. Price* A03

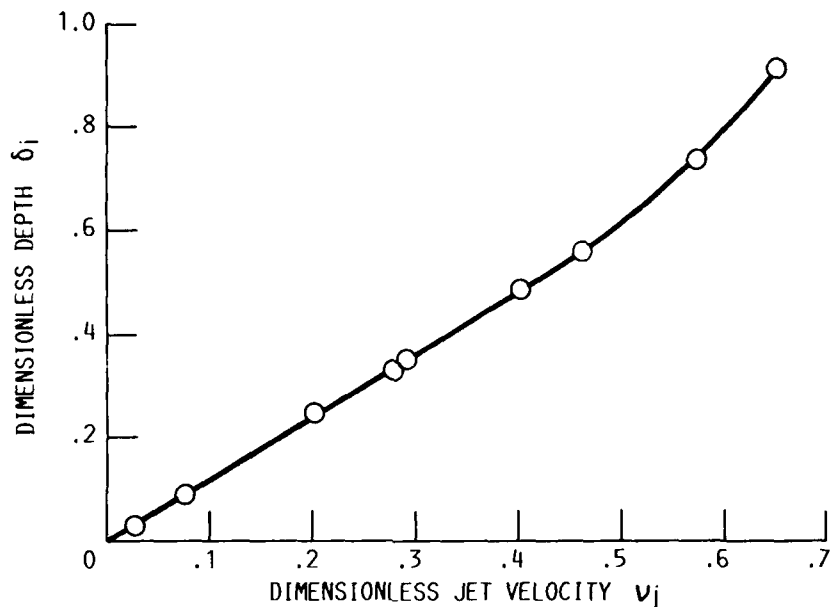


FIGURE 5. - DIMENSIONLESS  $\delta_j$  FOR A GIVEN DIMENSIONLESS JET VELOCITY  $v_j$  (AT OPTIMUM VALUE FOR ALPHA)  $\alpha = 47^\circ$ , PRESSURE ANGLE,  $20^\circ$ ; NUMBER OF TEETH, 28; 8 DIAMETRIAL PITCH.

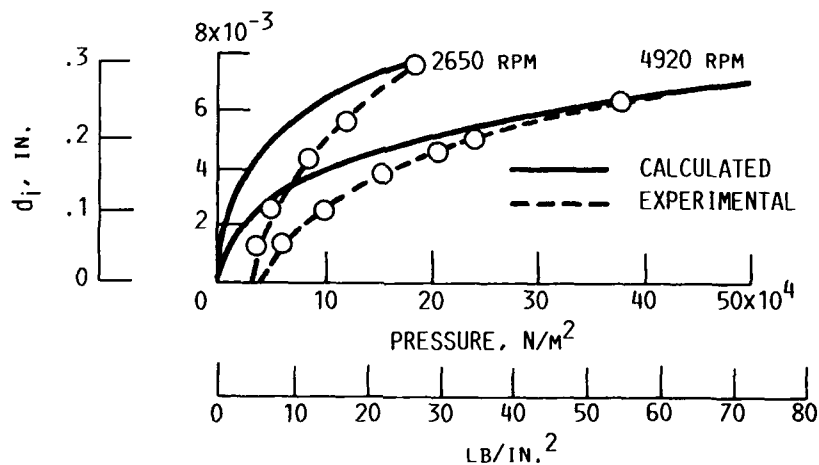


FIGURE 6. - CALCULATED AND EXPERIMENTAL IMPINGEMENT DEPTH VERSUS OIL JET PRESSURE AT 4920 AND 2560 RPM.